Unmixing hyperspectral images using Markov random fields

Olivier Eches, Nicolas Dobigeon and Jean-Yves Tourneret

University of Toulouse, IRIT/INP-ENSEEIHT, 2 rue Camichel, 31071 Toulouse cedex 7, France

Abstract. This paper proposes a new spectral unmixing strategy based on the normal compositional model that exploits the spatial correlations between the image pixels. The pure materials (referred to as *endmembers*) contained in the image are assumed to be available (they can be obtained by using an appropriate endmember extraction algorithm), while the corresponding fractions (referred to as *abundances*) are estimated by the proposed algorithm. Due to physical constraints, the abundances have to satisfy positivity and sum-to-one constraints. The image is divided into homogeneous distinct regions having the same statistical properties for the abundance coefficients. The spatial dependencies within each class are modeled thanks to Potts-Markov random fields. Within a Bayesian framework, prior distributions for the abundances and the associated hyperparameters are introduced. A reparametrization of the abundance coefficients is proposed to handle the physical constraints (positivity and sum-to-one) inherent to hyperspectral imagery. The parameters (abundances), hyperparameters (abundance mean and variance for each class) and the classification map indicating the classes of all pixels in the image are inferred from the resulting joint posterior distribution. To overcome the complexity of the joint posterior distribution, Markov chain Monte Carlo methods are used to generate samples asymptotically distributed according to the joint posterior of interest. Simulations conducted on synthetic and real data are presented to illustrate the performance of the proposed algorithm.

Keywords: Bayesian inference, Monte Carlo methods, spectral unmixing, hyperspectral images.
MSC: 62F15 Bayesian Inference; 65C05 Monte Carlo methods; 68U10 Image processing.

1. INTRODUCTION

Spectral unmixing is a key issue in hyperspectral image analysis and therefore has received considerable attention in the signal and image processing literature (see for instance [1] and references therein). The linear mixing model (LMM) assumes that an image pixel is the linear combination of a given number R of pure deterministic spectra, known as *endmembers*, weighted by their corresponding fractions, known as *abundances* [1]. The first step of unmixing consists of recovering the endmember spectral signatures using an endmember extraction algorithm (EEA) such as the N-FINDR [2]. Note that these two steps can be done jointly as in [3]. The EEA step is then followed by the so-called *inversion* step where the abundances are estimated. Due to obvious physical considerations, the abundances must satisfy positivity and sum-to-one constraints. Many algorithms have been developed for this LMM-based inversion step [1], [4], [5]. Recently, the normal compositional model (NCM) introduced in [6] has been proposed as an alternative of the LMM for a new Bayesian inversion algorithm [7]. The NCM assumes that the reflectance vector $\mathbf{y}_p = [y_{1,p}, \ldots, y_{L,p}]$ measured in L bands of a pixel p is a combination of random endmembers with known means (instead of deterministic and known ones with the LMM)

$$\mathbf{y}_p = \sum_{r=1}^{R} \mathbf{e}_r a_{r,p}, \tag{1}$$

CP1305, *Bayesian Inference and Maximum Entropy Methods in Science and Engineering*
edited by A. Mohammad-Djafari, J.-F. Bercher, and P. Bessière

where R is the number of pure materials in the pixel p, the $\mathbf{e}_1,\ldots,\mathbf{e}_R$ are independent Gaussian vectors and $a_{r,p}$ is the rth ($r=1,\ldots,R$) abundance coefficient of the pth pixel. As illustrated in [7], the NCM can be preferred to the LMM when the image does not contain enough pure pixels. A similar model to the NCM was proposed in [8] that estimates the endmember means while the endmember covariance are known.

Most inversion strategies have been developed in a pixel-by-pixel context. Consequently, they do not exploit the possible spatial dependance between the different pixels of the hyperspectral image. We propose in this paper to exploit the correlations between the pixel of the image to derive a new unmixing procedure. More precisely, we generalize the Bayesian unmixing algorithm developed in [7] to take into account spatial correlations between the pixels of an hyperspectral image. First, the image is partitioned into homogeneous regions. In each region, the abundance vectors are assumed to share the same first and second order moments (means and covariances). This implies an implicit image classification modeled by hidden labels whose spatial dependencies are modeled by a Potts-Markov random field [9], a particular case of Markov random fields (MRFs). Appropriate prior distributions with unknown means and variances depending on the pixel class are chosen for the abundance vectors. These abundances are reparametrized since the uniform prior distribution used in previous work (like in [4] or [7]) is not sufficiently flexible to allow ones an efficient image partitioning. The accuracy of the abundance estimation depends on the associated hyperparameters. We propose to estimate these hyperparameters in a fully unsupervised manner by introducing a second level of hierarchy in the Bayesian inference. Hyperparameters are then assigned non-informative prior distributions. The joint posterior distribution of the parameters and hyperparameters is then computed from the likelihood and these prior distributions. The resulting posterior is too complex to derive the classical Bayesian estimators such as the MMSE and MAP estimators. Thus we propose to use Markov chain Monte Carlo (MCMC) methods to generate samples asymptotically distributed according to the joint posterior. These samples are then used to estimate the unknown model parameters.

2. PROBLEM FORMULATION

2.1. Introducing spatial dependencies between the image pixels

This paper assumes that the abundances of a given pixel are *a priori* similar to the abundances of its neighboring pixels. Firstly, the image is divided into K regions or *classes*. In each class, the abundance vectors have the same mean and covariance matrix for all the pixels of the class. The subset $I_k \subset \{1,\ldots,P\}$ contains the indexes of the pixels that belong to the kth class. The vector $\mathbf{z}=[z_1,\ldots,z_P]^T$ where P is the total number of pixels and $z_p \in \{1,\ldots,K\}$ represents the hidden variables or *labels* that allow one to identify the class to which each pixel p belongs ($p=1,\ldots,P$), i.e., $z_p=k$ if and only if $p \in I_k$.

As explained above, the abundances have to satisfy positivity and sum-to-one constraints for each pixel p

$$\begin{cases} a_{r,p} \geq 0, \forall r=1,\ldots,R, \\ \sum_{r=1}^{R} a_{r,p}=1, \end{cases} \tag{2}$$

where $\mathbf{a}_p=[a_{1,p},\ldots,a_{R,p}]^T$ and R number of pure materials. This paper proposes to reparametrize the abundance coefficients by using random *logistic* coefficients $\mathbf{t}_p=[t_{1,p}\ldots,t_{R,p}]^T$ (see [10] and [11] for motivation)

$$a_{r,p}=\frac{\exp(t_{r,p})}{\sum_{r=1}^{R}\exp(t_{r,p})}. \tag{3}$$

This reparametrization ensures positivity and sum-to-one constraints for the abundances. In a given class k, a common Gaussian distribution (with mean vector $\boldsymbol{\psi}_k$ and covariance matrix σ_k^2) is chosen as prior for the logistic coefficients $\mathbf{t}_p$, relative to the pixels $p \in I_k$. Therefore, the class k is fully characterized by a mean vector $\boldsymbol{\psi}_k$ and a covariance matrix $\boldsymbol{\Sigma}_k$.

2.2. Likelihood

The NCM model assumes the endmember $\mathbf{e}_{p,r}$ ($r = 1,\ldots,R$, $p = 1,\ldots,P$) has a Gaussian distribution $\mathbf{e}_{p,r}|w_p^2 \sim \mathcal{N}\left(\mathbf{m}_r, w_p^2\mathbf{I}_L\right)$, with $\mathbf{m}_r$ known. Therefore the likelihood function of $\mathbf{y}_p$ can be expressed as

$$f\left(\mathbf{y}_p, |\mathbf{t}_p, w_p^2\right) = \frac{1}{\left[2\pi w_p^2 c(\mathbf{t}_p)\right]^{\frac{L}{2}}} \exp\left[-\frac{\|\mathbf{y}-\boldsymbol{\mu}(\mathbf{t}_p)\|^2}{2w_p^2 c(\mathbf{t}_p)}\right], \tag{4}$$

with

$$\boldsymbol{\mu}(\mathbf{t}_p) = \sum_{r=1}^{R} \mathbf{m}_r a_{r,p}(\mathbf{t}_p), \quad c(\mathbf{t}_p) = \sum_{r=1}^{R} a_{r,p}^2(\mathbf{t}_p),$$

and $\|\mathbf{x}\| = \sqrt{\mathbf{x}^T\mathbf{x}}$ is the standard ℓ_2 norm. By assuming independence between the different observed spectra, the likelihood of the P image pixels is

$$f(\mathbf{Y}|\mathbf{T},\mathbf{w}) = \prod_{p=1}^{P} f\left(\mathbf{y}_p|\mathbf{t}_p, w_p^2\right). \tag{5}$$

2.3. Parameter priors

The unknown parameter vector associated to the NCM unmixing strategy is defined as $\boldsymbol{\Theta} = \{\mathbf{T},\mathbf{z},\mathbf{w}\}$, where $\mathbf{w} = \left[w_1^2,\ldots,w_P^2\right]^T$ is the endmember variance vector, $\mathbf{z}$ is the label vector and $\mathbf{T} = [\mathbf{t}_1,\ldots,\mathbf{t}_P]$ with $\mathbf{t}_p = [\mathbf{t}_{1,p},\ldots,\mathbf{t}_{R,p}]^T$ $(p = 1,\ldots,P)$ is the logistic coefficient matrix used for the abundance reparametrization. This section introduces the prior distributions of the unknown parameters and their associated hyperparameters in the proposed hierarchical Bayesian framework.

Label prior. The spatial correlation between the image pixels can be represented by using MRFs. MRFs allow one to define a symmetric relation between one pixel and its nearby neighbors through the use of the labels. More specifically, the prior distribution of the label vector $\mathbf{z} = [z_1,\ldots,z_P]^T$ is a Potts-Markov random field, as in [12]. Considering a pixel p and its 4 nearby neighbors (first order neighborhood), the resulting prior distribution for the label vector can be written as

$$f(\mathbf{z}) \propto \exp\left[\beta \sum_{p=1}^{P} \sum_{p' \in \mathcal{V}(p)} \delta(z_p - z_{p'})\right], \tag{6}$$

where $\propto$ means "proportional to", $\mathcal{V}(p)$ is the first order neighborhood, β is the *granularity* coefficient (assumed to be known in this study) and $\delta(\cdot)$ is the Kronecker function

$$\delta(x) = \begin{cases} 1, & \text{if } x = 0, \\ 0, & \text{otherwise.} \end{cases}$$

Logistic coefficient prior. For a given pixel p and by assuming independence between the logistic coefficients $t_{1,p},\ldots,t_{R,p}$, the prior distribution for the vector $\mathbf{t}_p = [t_{1,p},\ldots,t_{R,p}]^T$ is the following Gaussian distribution

$$f(\mathbf{t}_p|z_p = k,\boldsymbol{\psi}_k,\boldsymbol{\Sigma}_k) \sim \mathcal{N}(\boldsymbol{\psi}_k,\boldsymbol{\Sigma}_k) \tag{7}$$

parameterized by the mean vector $\boldsymbol{\psi}_k = [\psi_{1,k},\ldots,\psi_{R,k}]^T$ and by the $R \times R$ diagonal covariance matrix $\boldsymbol{\Sigma}_k = \text{diag}\left(\sigma^2_{r,k}\right)$ whose diagonal elements are $\sigma^2_{r,k}$ for $r = 1,...,R$. Note that the mean vector $\boldsymbol{\psi}_k$ and the covariance matrix $\boldsymbol{\Sigma}_k$ of the logistic coefficient vector $\mathbf{t}_p$ both depend on the region k. By assuming prior independence between the P vectors $\mathbf{t}_1,\ldots,\mathbf{t}_P$, the full posterior distribution for the logistic coefficient matrix $\mathbf{T}$ is

$$f(\mathbf{T}|\boldsymbol{\Psi},\boldsymbol{\Sigma}) = \prod_{k=1}^{K}\prod_{p\in I_k} f(\mathbf{t}_p|z_p = k,\boldsymbol{\psi}_k,\boldsymbol{\Sigma}_k), \tag{8}$$

with $\boldsymbol{\Psi} = [\boldsymbol{\psi}_1,\ldots,\boldsymbol{\psi}_K]$ and $\boldsymbol{\Sigma} = \{\boldsymbol{\Sigma}_1,\ldots,\boldsymbol{\Sigma}_K\}$.

Endmember variance prior. A conjugate inverse gamma distribution is assigned to the pth endmember variance

$$w_p^2|\kappa \sim IG(\nu,\kappa), \tag{9}$$

where ν and κ are adjustable hyperparameters. In the sequel, ν will be fixed ($\nu = 1$) and κ will be estimated as in [13]. Assuming independence between the endmember variances w_p^2 ($p = 1,\ldots,P$), the full prior distribution for $\mathbf{w} = \left[w_1^2,\ldots,w_P^2\right]^T$ can be expressed as

$$f(\mathbf{w}|\kappa) = \prod_{p=1}^{P} f\left(w_p^2|\kappa\right) \tag{10}$$

2.4. Hyperparameter priors

This paper proposes to define prior distributions for the logistic coefficient means $\psi_{r,k}$ and variances $\sigma^2_{r,k}$ as conjugate Gaussian and inverse-gamma distributions, i.e.,

$$\begin{array}{c} \psi_{r,k}|\upsilon^2 \sim \mathcal{N}\left(0,\upsilon^2\right) \\ \sigma^2_{r,k}|\xi,\gamma \sim IG(\xi,\gamma) \end{array} \tag{11}$$

where υ^2 is an adjustable hyperparameter and ξ and γ have been fixed to $\xi = 1$ and $\gamma = 5$ (to obtain a large variance). Jeffreys' priors are also assigned to the hyperparameters κ and υ^2 defined as

$$f(\kappa) \propto \frac{1}{\kappa}\mathbf{1}_{\mathbb{R}^+}(\kappa), \quad f(\upsilon^2) \propto \frac{1}{\upsilon^2}\mathbf{1}_{\mathbb{R}^*}(\upsilon^2). \tag{12}$$

By assuming *a priori* independence between the individual hyperparameters, the full hyperprior can be obtained for the hyperparameter vector $\Omega = \left\{\boldsymbol{\Psi},\boldsymbol{\Sigma},\upsilon^2,\kappa\right\}$

$$f(\Omega) \propto f(\kappa)f(\upsilon^2)\prod_{k=1}^{K}\prod_{r=1}^{R} f(\psi_{r,k}|\upsilon^2)f(\sigma^2_{r,k}). \tag{13}$$

2.5. Joint distribution

The likelihood and the priors defined above allow one to express the joint posterior distribution using the hierarchical structure

$$
\begin{aligned}
f(\boldsymbol{\Theta},\Omega|\mathbf{Y}) \propto & \prod_{p=1}^{P} \frac{1}{\left[w_p^2 c(\mathbf{t}_p)\right]^{L/2}} \exp\left[-\sum_{p=1}^{P} \frac{\|\mathbf{y}_p - \boldsymbol{\mu}(\mathbf{t}_p)\|^2}{2w_p^2 c(\mathbf{t}_p)}\right] \\
& \times \exp\left[\sum_{p=1}^{P} \sum_{p' \in \mathcal{V}(p)} \beta\delta(z_p - z_{p'})\right] \kappa^{P-1} \prod_{p=1}^{P} \left(\frac{1}{w_p^2}\right)^{\nu+1} \exp\left(-\frac{\kappa}{w_p^2}\right) \left(\frac{1}{\upsilon^2}\right)^{\frac{RK}{2}+1} \\
& \times \prod_{r,k} \frac{1}{\sigma_{r,k}^{n_k+1}} \exp\left[-\left(\frac{\psi_{r,k}^2}{2\upsilon^2} + \frac{2\gamma + \sum_{p \in I_k} (t_{r,p} - \psi_{r,k})^2}{2\sigma_{r,k}^2}\right)\right]
\end{aligned}
\tag{14}
$$

with $n_k = \text{card}(I_k)$. This posterior distribution is too complex to derive closed-form expressions for the MMSE and MAP estimators of $\boldsymbol{\Theta}$. A possible solution to this issue is the use of MCMC methods. More precisely, a hybrid Gibbs sampler is proposed to generate samples that are asymptotically distributed according to $f(\boldsymbol{\Theta},\Omega|\mathbf{Y})$. The samples are then used to approximate the Bayesian estimators.

3. HYBRID GIBBS SAMPLER

The principle of the Gibbs sampler is to iteratively generate samples distributed according to the conditional distributions of the parameters [14]. This section derives the conditional distributions associated to (14).

Conditional distribution of the label vector $\mathbf{z}$. For each pixel p ($p = 1,\ldots,P$), the class label z_p is a discrete random variable whose conditional distribution is fully characterized by the probabilities denoted as

$$
\begin{aligned}
\mathrm{P}\left[z_p = k|\mathbf{z}_{\text{-}p}, \mathbf{t}_p, \boldsymbol{\psi}_k, \boldsymbol{\Sigma}_k\right] \propto & |\boldsymbol{\Sigma}_k|^{-1/2} \exp\left[-\frac{1}{2}(\mathbf{t}_p - \boldsymbol{\psi}_k)^T \boldsymbol{\Sigma}_k^{-1} (\mathbf{t}_p - \boldsymbol{\psi}_k)\right] \\
& \times \exp\left[\sum_{p=1}^{P} \sum_{p' \in \mathcal{V}(p)} \beta\delta(z_p - z_{p'})\right]
\end{aligned}
\tag{15}
$$

with $|\boldsymbol{\Sigma}_k| = \prod_{r=1}^{R} \sigma_{r,k}^2$, $k = 1,\ldots,K$ (K is the number of classes) and $\mathbf{z}_{\text{-}p}$ denotes the vector $\mathbf{z}$ whose pth element has been removed. The parameter K is assumed to be known in this study (see [11] for discussion about its estimation). Since this distribution is discrete, the samples are drawn by generating a discrete value $k \in \{1,\ldots,K\}$ with the probabilities (15) as explained in [15].

Conditional distribution of logistic coefficient matrix $\mathbf{T}$. For a given pixel p, the conditional distribution of $\mathbf{t}_p$ is

$$f\left(\mathbf{t}_p|z_p=k,\boldsymbol{\psi}_k,\boldsymbol{\Sigma}_k,\mathbf{y}_p,s_p^2\right)\propto\left(\frac{1}{s_p^2}\right)^{\frac{L}{2}}\exp\left\{-\frac{1}{2s_p^2}\left\|\mathbf{y}_p-\mathbf{M}\mathbf{a}_p(\mathbf{t}_p)\right\|^2\right\}$$
$$\times\left|\boldsymbol{\Sigma}_k\right|^{-\frac{1}{2}}\exp\left[-\frac{1}{2}\left(\mathbf{t}_p-\boldsymbol{\psi}_k\right)^T\boldsymbol{\Sigma}_k^{-1}\left(\mathbf{t}_p-\boldsymbol{\psi}_k\right)\right]. \quad (16)$$

Generating samples according to this posterior distribution can be achieved by using Metropolis-Hastings step with a Gaussian proposal distribution as proposal distribution, following the strategy detailed in [15].

Conditional distributions of the endmember variances. Considering each pixel p, the following inverse-Gamma distribution is obtained for w_p^2

$$w_p^2|\mathbf{y}_p,\mathbf{t}_p,\kappa\sim I\mathcal{G}\left(\frac{L}{2}+1,\frac{\left\|\mathbf{y}_p-\boldsymbol{\mu}(\mathbf{t}_p)\right\|^2}{2c(\mathbf{t}_p)}+\kappa\right). \quad (17)$$

Conditional distributions of $\boldsymbol{\Psi}$ *and* $\boldsymbol{\Sigma}$. For each endmember r ($r=1,\ldots,R$) and each class k ($k=1,\ldots,K$) and by denoting $\bar{t}_{r,k}=\frac{1}{n_k}\sum_{p\in I_k}t_{r,p}$, the conditional distributions of $\psi_{r,k}$ and $\sigma_{r,k}^2$ can be written as

$$\psi_{r,k}|\mathbf{z}=k,\mathbf{t}_r,\sigma_{r,k}^2,\upsilon^2\sim\mathcal{N}\left(\frac{\upsilon^2 n_k\bar{t}_{r,k}}{\sigma_{r,k}^2+\upsilon^2 n_k},\frac{\upsilon^2\sigma_{r,k}^2}{\sigma_{r,k}^2+\upsilon^2 n_k}\right) \quad (18)$$

$$\sigma_{r,k}^2|\mathbf{z}=k,\mathbf{t}_r,\psi_{r,k}\sim I\mathcal{G}\left(\frac{n_k}{2}+1,\gamma+\sum_{p\in I_k}\frac{\left(t_{r,p}-\psi_{r,k}\right)^2}{2}\right). \quad (19)$$

Conditional distributions of υ^2 *and* κ. The conditional distributions of υ^2 and κ are the following inverse-Gamma and Gamma distributions, respectively

$$\upsilon^2|\boldsymbol{\Psi}\sim I\mathcal{G}\left(\frac{RK}{2},\frac{1}{2}\sum_{k=1}^{K}\boldsymbol{\psi}_k{}^T\boldsymbol{\psi}_k\right),\quad \kappa|\mathbf{s}\sim\mathcal{G}\left(P,\sum_{p=1}^{P}\frac{1}{s_p^2}\right). \quad (20)$$

The proposed Gibbs sampler iteratively generates N_{MC} samples distributed according to the different conditional distributions described above. The first generated samples N_{bi} belonging to the so-called *burn-in* period are ignored whereas the last samples are employed to estimate the unknown model parameters and hyperparameters. More precisely, we estimate the labels using the MAP estimator approximated by retaining the samples that maximizes the conditional distribution of $\mathbf{z}$. Then, each abundance vector is estimated conditionally to the MAP estimates of its label by averaging the last samples associated to the corresponding pixel (following the MMSE principle).

TABLE 1. Actual and estimated abundance means for each class.

	Class 1	Class 2	Class 3
	$\boldsymbol{\mu}_1 = \mathrm{E}[\mathbf{a}_p]$	$\boldsymbol{\mu}_2 = \mathrm{E}[\mathbf{a}_p]$	$\boldsymbol{\mu}_3 = \mathrm{E}[\mathbf{a}_p]$
Real values	$[0.6, 0.3, 0.1]^T$	$[0.3, 0.5, 0.2]^T$	$[0.3, 0.2, 0.5]^T$
Estimates	$[0.59, 0.29, 0.12]^T$	$[0.31, 0.49, 0.2]^T$	$[0.31, 0.2, 0.49]^T$

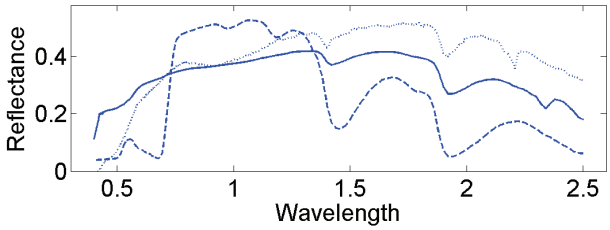

FIGURE 1. The $R = 3$ endmember spectra: construction concrete (solid line), green grass (dashed line), micaceous loam (dotted line).

4. SIMULATION RESULTS ON SYNTHETIC DATA

To analyze the performance of our algorithm, a 25×25 synthetic image with $K = 3$ classes was considered. The image contains $R = 3$ mixed components whose spectra ($L = 413$ spectral bands) are construction concrete, green grass and micaceous loam (extracted from ENVI software library). These spectra are represented in Fig. 1.

A label map, shown Fig. 2 (left) was generated using a Potts-Markov random field with $\beta = 1.1$. Then, the abundance means have been fixed for each class as reported in Table 1. The generated abundance maps for the NCM are depicted in Fig. 3 (left). Note that a black (resp. white) pixel indicates a weak (resp. strong) value of the abundance coefficient. The endmember variance was generated according to its prior distribution with $\kappa = 1 \times 10^{-3}$, leading to a signal-to-noise ratio of 12dB. A number of $N_{\mathrm{MC}} = 5000$ iterations (with 500 burn-in iterations) was chosen for all results.

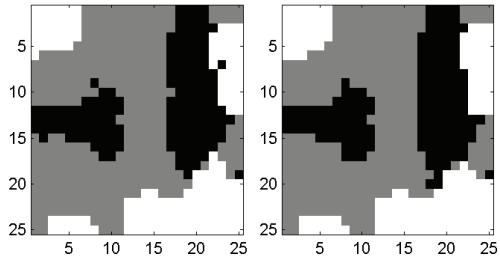

FIGURE 2. Left: Actual label map. Right: label map estimated by the proposed hybrid Gibbs sampler.

The MAP estimates of the label vector $\mathbf{z}$ are shown on Fig. 2 (right) and the MMSE estimates of the abundance vectors (conditionally upon the label MAP estimates) are represented in Fig. 3 (right). The estimated abundance means and variances for each endmember in each class have been reported in Table 1 showing the good performance of the algorithm. Note that the execution time of this simulation on a Core(TM)2Duo 2.66GHz was about 26 minutes. Comparisons with previous unmixing results with fixed endmembers and $K = 1$ are reported in [11].

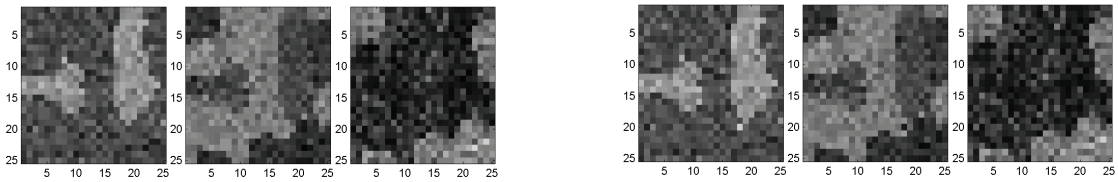

FIGURE 3. Left: abundance maps of the 3 pure materials for NCM. Right: estimated abundance maps of the 3 pure materials from the NCM hybrid Gibbs sampler (from left to right: construction concrete, green grass, micaceous loam).

5. CONCLUSIONS

A new spectral unmixing strategy was developed taking into account the possible spatial correlation between the pixels of an hyperspectral image. Hidden variables (labels) were introduced to identify the classes resulting from the image partitioning. These abundances of each class were assumed to share the same first and second order statistics. After a reparametrization of the abundances, the joint posterior distribution of the unknown parameters and hyperparameters was derived. We proposed to generate samples according to this posterior distribution using an hybrid Gibbs sampler and to use these samples to estimate the image labels and the abundances (conditionally upon the label estimates). The results obtained on simulated data are interesting. This algorithm has also been applied on real data (see [15] for more details). The estimation of the granularity coefficient involved in Potts-Markov random fields is currently under investigation.

REFERENCES

1. N. Keshava, and J. Mustard, *IEEE Signal Processing Magazine* pp. 44–56 (2002).
2. M. E. Winter, "Fast Autonomous Spectral Endmember Determination in Hyperspectral Data," in *Proc. 13th Int. Conf. on Applied Geologic Remote Sensing*, Vancouver, 1999, vol. 2, pp. 337–344.
3. N. Dobigeon, S. Moussaoui, M. Coulon, J.-Y. Tourneret, and A. O. Hero, *IEEE Trans. Signal Processing* **57**, 4355–4368 (2009).
4. N. Dobigeon, J.-Y. Tourneret, and C.-I Chang, *IEEE Trans. Signal Processing* **56**, 2684–2696 (2008).
5. D. C. Heinz, and C.-I Chang, *IEEE Trans. Geosci. and Remote Sensing* **39**, 529–545 (2001).
6. M. T. Eismann, and D. Stein, "Stochastic Mixture Modeling," in *Hyperspectral Data Exploitation: Theory and Applications*, edited by C.-I Chang, Wiley, 2007, chap. 5.
7. O. Eches, N. Dobigeon, C. Mailhes, and J.-Y. Tourneret, *IEEE Trans. Image Processing* **19**, 1403–1413 (2010).
8. A. Zare, and P. Gader, *IEEE Trans. Geosci. and Remote Sensing* **48**, 2620–2632 (2010).
9. F. Wu, *Rev. Modern Phys.* **54**, 235–268 (1982).
10. A. Gelman, F. Bois, and J. Jiang, *J. Amer. Math. Soc.* **91**, 1400–1412 (1996).
11. O. Eches, N. Dobigeon, and J.-Y. Tourneret, Enhancing hyperspectral image unmixing with spatial correlations, Tech. rep., University of Toulouse (2010), URL `http://eches.perso.enseeiht.fr`.
12. N. Bali, and A. Mohammad-Djafari, *IEEE Trans. Image Processing* **17**, 217–225 (2008).
13. N. Dobigeon, J.-Y. Tourneret, and M. Davy, *IEEE Trans. Signal Processing* **55**, 1251–1263 (2007).
14. C. P. Robert, and G. Casella, *Monte Carlo Statistical Methods*, Springer Verlag, New York, 2004.
15. O. Eches, N. Dobigeon, and J.-Y. Tourneret, *IEEE Trans. Geosci. and Remote Sensing* (2010), URL `http://arxiv.org/abs/1002.1059`, submitted.